Letter

Observations on the microstructure of Hot-pressed silicon nitride

Fabrication of silicon nitride shapes by hot-pressing gives a product whose density and mechanical properties are markedly superior to those of reaction bonded material. Moreover, it has been found empirically that high density and strength are obtained only when a small quantity of fluxing agent, usually MgO, is mixed with the silicon nitride powder prior to hot-pressing [1]. The influence of MgO on the chemical reactions and mechanism of densification during the hot-pressing cycle has been identified in recent work by Wild *et al.* [2].

The present note describes some of the microstructural characteristics of β-silicon nitride produced by hot pressing. Commercial powder containing $\nless$ 93 wt% of the α-phase with an approximate composition $Si_{11 \cdot 5}N_{15}O_{0 \cdot 5}$ [3], and $\ngtr$ 7 wt% of β-Si_3N_4 was mixed with 5 wt% MgO and hot-pressed at 1750°C under a pressure of 3000 psi*. X-ray examination of the product using a Hägg-Guinier focusing camera showed ~ 95% β-silicon nitride with small quantities of silicon carbide.

Figure 1 Replica from section normal to hot-pressing direction (× 5000).

The microstructures of hot-pressed samples were studied on a Philips 300 electron microscope using both the replica and thin foil techniques. Standard metallographic methods were used to prepare shadowed carbon replicas and the thin foils were obtained by ion-beam thinning.

A typical region of the microstructure from a section perpendicular to the hot-pressing direction is shown in the surface replica, Fig. 1; a significant feature is the small but extremely variable grain size, ranging from ~ 0.1 to 5.0 μm. In addition, the grain shape varied in terms of aspect ratio on a planar section from a value ~ 1.0 (equiaxed) to values as high as 10. It was noticeable that in any one replica a significant fraction of non-equiaxed grains were elongated along approximately the same axis, as indicated in Fig. 1.

The observation of regions of anisotropic grain shape suggested that the β-silicon nitride might also show a crystallographic preferred orientation. This possibility was investigated by comparing peak intensities on X-ray diffractometer traces taken from sections parallel and perpendicular to the direction of hot-pressing. The X-ray intensities for a selection of planes measured in arbitrary units, are shown in Table I, together with the relative intensities for a random powder of β-Si_3N_4 taken from the ASTM index. For both sections, the peak intensities are clearly different from those expected for a crystallographically random hot pressing. Of particular significance is the decrease in

TABLE I

Reflection (*hkl*)	Intensity* (arbitrary units) Parallel section	Normal section	I/I_0 (ASTM)
200	75	69	85
101	157	28	100
210	77	70	100
201	30	11	35
301	30	15	70
002	19	4	35
321	30	20	40

*Background subtracted.

---

*10^3 psi = 6.89 Nmm^{-2}

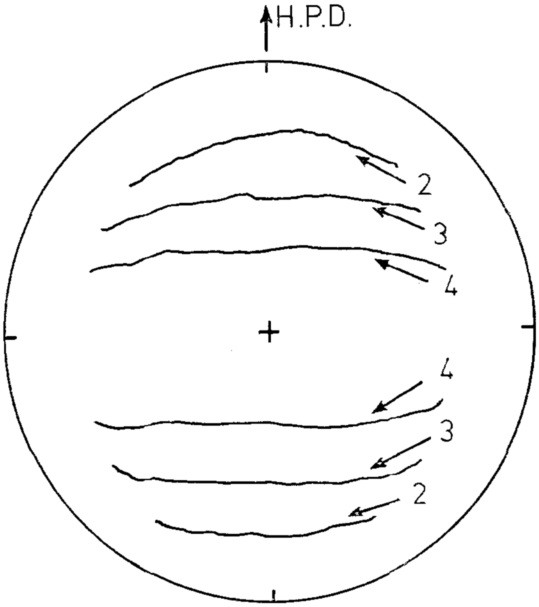

Figure 2 {101} pole figure from section parallel to hot-pressing direction (HPD); intensities in arbitrary units.

intensity from planes which intersect the c-axis of the β-Si_3N_4 hexagonal unit cell (i.e. reflections with an l index) in the section normal to the hot-pressing direction. This decrease is quite marked as can be seen by the change in the ratio $I_{(101)}/I_{(210)}$ from 2 to ~ 0.5 in sections parallel and normal to the hot-pressing direction respectively. The results suggest that the c-axis has a preferred orientation perpendicular to the hot-pressing direction.

A texture goniometer and the standard Schulz reflection method [4] were used in an attempt to describe the preferred orientation more precisely by means of pole figure determination. In general these results were consistent with the peak intensity measurements, as shown by the {101} pole figure for the parallel section, Fig. 2. The distribution of basal planes was difficult to measure directly because of their relatively weak intensity. However, since the angle between {101} and {002} is only 24° (c/a for β-Si_3N_4 is 0.383), it is reasonable to suppose that the preferred orientation of basal planes is similar to that in Fig. 2, i.e. a band of higher intensity across the central region of the pole figure. A more quantitative description of the pole distribution was not possible, mainly because the texture was not sufficiently pronounced.

Transmission electron microscopy, Fig. 3a to d, confirmed the microstructural characteristics observed on replicas, and revealed further important features. The main one was the observation of a significantly higher volume fraction of fine grains (< 0.5 μm) than is apparent from the replicas. This discrepancy is probably due to the etching technique failing to reveal completely the microstructure, particularly sub-grains, prior to replication. Tilting experiments demonstrated that many of the sub-micron grains were bounded by low-angle boundaries.

A second important constituent was a network of second phase particles, arrowed in Fig. 3b, generally located at grain boundaries, which were clearly evident due to their resistance to ion thinning. The origin and composition of this second phase is uncertain, but since the volume fraction is significant (1 to 5%), one possibility is the silicon carbide identified by X-ray diffraction.

There is evidence that an amorphous phase is formed during the hot-pressing of Si_3N_4 which plays an important role in the mechanism of densification and also accounts for the marked decrease in high temperature strength of the hot-pressed product [2]. Although there was no indication of a continuous grain-boundary film, regions were frequently observed which showed no diffraction effects or variations in transmitted electron intensity on specimen tilting; such regions invariably enveloped a number of β–Si_3N_4 grains, Fig. 3c. Since the most likely site for any amorphous reaction product would be the interface between the original α-Si_3N_4 particles and since the phase transformation $\alpha \rightarrow \beta$ occurs during hot-pressing, there is no reason to expect a glassy phase at all grain boundaries. Therefore, regions such as those in Fig. 3c could be an amorphous phase and, because they are located at the junctions of several grains, could accommodate relative particle movement during hot-pressing.

In agreement with previous work [5] dislocations were commonly found in many grains and probably arise due to plastic deformation during pressing or from phase transformation stresses. Helical dislocations and loops were occasionally observed, usually associated with inclusions, and appeared to be punched out due to differential contraction stresses during cooling, Fig. 3d.

The microstructural observations are consistent with recent ideas on the mechanism of densification during the hot-pressing of silicon nitride [2]. In absence of comparison with the

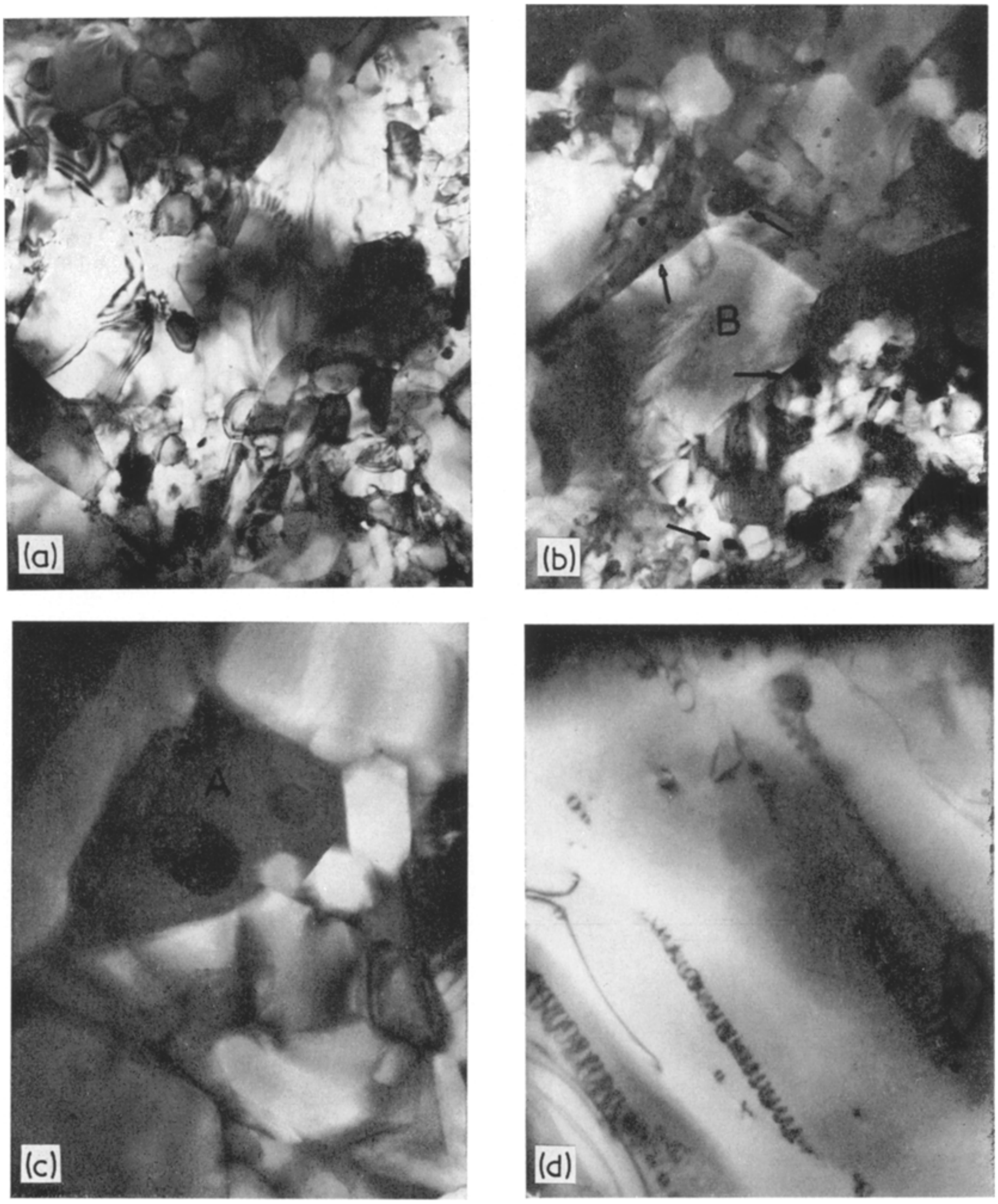

Figure 3 Transmission electron micrographs showing (a) general microstructural features (× 10 000), (b) second phase particles, arrowed (× 10 000), (c) amorphous region, marked A (× 30 000), (d) helical dislocations and loops (× 20 000).

α starting material, the sub-micron grain size of β cannot support the suggestion that grain refinement occurs during the α-β phase transformation, but the presence of relatively large grains (e.g. B in Fig. 3b) probably represents the β-Si_3N_4 particles in the original powder. The wide variations in grain size and the dispersion of second phase, possibly silicon carbide, is likely to be important in limiting the low temperature strength achieved in hot-pressed material. Moreover, the anisotropy of grain shape and the crystallographic preferred orientation, which appear to be related phenomena, have been shown to introduce marked directionality of physical and mechanical properties in hot-pressings of Si_3N_4 [6]. Further microstructural investigation is required to establish clearly the quantity and distribution of the amorphous constituent.

Acknowledgements

The authors wish to thank Joseph Lucas Ltd for the supply of hot-pressed silicon nitride, Dr G. W. Lorimer for assistance with the ion-thinning, and International Research and Development Ltd for the use of a texture goniometer. They are also grateful to Professor K. H. Jack for valuable advice and discussion.

References

1. G. G. DEELEY, J. M. HERBERT, and N. C. MOORE, *Powder Met.* **1** (1961) 145.
2. S. WILD, P. GRIEVESON, K. H. JACK, and M. S. LATIMER, *Special Ceramics* **5** (1972) 377.
3. S. WILD, P. GRIEVESON, and K. H. JACK, *ibid* **5** (1972) 385.
4. L. G. SCHULZ, *J. Appl. Phys.* **20** (1949) 1030.
5. A. G. EVANS and J. V. SHARP, *J. Mater. Sci.* **6** (1971) 1292.
6. F. F. LANGE, ASME publication 72-GT-56.

Received 13 September
and accepted 27 November 1973

K. NUTTALL*
D. P. THOMPSON
Wolfson Research Group for High-Strength Materials,
Crystallography Laboratory, Department of Metallurgy, The University,
Newcastle upon Tyne, UK

*Now at Atomic Energy of Canada Ltd, Whiteshell Nuclear Research Establishment, Pinawa, Manitoba, Canada.

Electrochemical aspects of dielectric breakdown in alkali halides

In metal-insulator-metal sandwiches involving alkali halides, it is found that an application of a suitable voltage (i.e. field) across the sandwich gives rise to the decomposition of the insulator [1]. In an alkali halide MX, the reaction at the anode is

$$X^- + \text{Anode} \rightarrow \tfrac{1}{2} X_2 + e + \text{Anode} \qquad (1)$$

where X_2 is the molecular halogen gas. The corresponding cathodic reaction may thus be written as

$$e_{\text{cathode}} + \square_{\text{insulator}} \rightarrow \square^{-}_{\text{insulator}} . \qquad (2)$$

Greene *et al* [1] have noted that for the "forming" (ie. electrolysis) to occur, the forming voltage, V_F, must just exceed, ΔG, the free energy change involved in the overall electrolysis reaction, presumably because

$$\Delta G = -nFE_0 \qquad (3)$$

where E_0 is the electrode potential (i.e. reversible) of the electrolysis reaction to which ΔG refers; n is the number of charge carriers transferred in the overall reaction and F is the Faraday. For electrolysis to occur, V_f must exceed E_0 (and hence ΔG) because some overpotential must be developed before the electrolysis can occur.

This note attempts to correlate the V_f values of these alkali halides to their band gaps, E_g values. Also, the relation of these considerations to the experimental values of the dielectric breakdown field for several alkali halides [2] will also be examined.

Since for the solid-state electrolysis to commence, the (exothermic) free energy of formation of the insulator must be just exceeded by the formation voltage [1] it follows that

$$eV_f \simeq -\Delta G \qquad (4)$$

where V_f is the forming voltage of the insulator, e is the electronic charge and ΔG is its free energy of formation per mole. For the alkali halides, ΔG per *mole* is the same thing as ΔG_e, the free energy of formation per *equivalent* which may also be approximated as the heat of formation per equivalent, ΔH_e, so that*

$$V_f \simeq -\Delta G \simeq -\Delta G_e \simeq -\Delta H_e . \qquad (5)$$

Now, it may be noted that [3, 4]

$$E_g \simeq 2(-\Delta H_e) \qquad (6)$$

where E_g is the band gap of the compound, the

**Notes:* 1. Since alkali halide are uni-univalent, ΔG/mole $= \Delta G_e$.
2. Since alkali halides are solids, entropy would be a rather negligible part of ΔG_e; for condensed phases in general, entropy considerations are relatively unimportant.